http://dx.doi.org/10.21611/qirt.2012.317

QIRT 2012

11th International Conference on
Quantitative InfraRed Thermography

Unsteady data reduction techniques for IR heat flux measurements: considerations of temporal and spatial resolution

by F. Schrijer

Delft University of Technology, Kluyverweg 1, 2629HS Delft The Netherlands, f.f.j.schrijer@tudelft.nl

Abstract

The effect of limited temporal resolution and lateral conduction on transient heat flux measurements by means of IR thermography is investigated. In combination three methods are compared that are based on 1D and 2D heat conduction models where the latter are capable of correcting for lateral conduction. It is found that for a constant heat flux without measurement noise 5 to 6 measurement points are sufficient to make a reliable estimate (<1%) of the heat flux. Furthermore it is shown that heat flux features having typical spatial wavelengths that are smaller than 3.5 times the penetration depth are modulated when evaluated by 1D methods that do not take into account lateral conduction. Finally an experimental data set is used to further investigate the above-mentioned effects, however not all theoretical observations could be confirmed indicating the need for further investigation by including a non-constant heat flux and measurement noise.

1. Introduction

Over the recent years infrared cameras using FPA sensors have become available commercially. Due to their increased digital resolution (total number of pixels per frame), higher acquisition speeds and improved NETD they represented an improvement with respect to the single detector systems with an opto-mechanical scanning system. Although the FPA systems offer many benefits over single detector system, additional sources of uncertainty and error due to the larger sensor size (sensor non-uniformity, optical aberrations) and more complicated read-out circuitry (ghosting) could be identified, causing the single detector system to remain the preferred choice for purists. For an overview of the performance and specific characteristics of FPA IR cameras the reader is referred to the papers of Pron and Bissieux (2004), Levesque et al. (2005) and Poncelet et al. (2011).

In this paper data processing techniques are discussed that are use for unsteady problems where the convective heat flux is obtained from the transient surface temperature signal. This approach is typically used in the field of fluid mechanics and aerospace studies where the temperature difference between the flow and model surface is used as the driving potential. Within this field one of the most important applications is the investigation of supersonic and hypersonic flows, which are generally characterized by relatively short measurement times (in the order of milliseconds to seconds) due to flow facility limitations.

Especially for these applications the increase in performance of FPA's expressed in terms of full frame acquisition frequency has significantly improved the measurement capabilities. Previously single detector with scanning systems operated at typical full frame frequencies ranging from 10 to 20 *Hz*, which are therefore not being able to capture the thermal transient. While the current FPA cameras can operate at full frame frequencies ranging from 100 to 200 *Hz* depending on the camera resolution allowing for an adequate sampling of the transient. Furthermore the FPA systems do no longer suffer from the inherent problem of scanning systems due to the continuously moving IFOV causing spatial modulation (de Luca and Cardone, 1991). However the modulation effects due to lateral conduction must be still considered.

In this paper two aspects of unsteady data reduction procedures are discussed that are pertinent for heat transfer investigations performed in short duration facilities. First is the effect of limited temporal resolution: combining a short test time (order of 0.1 seconds) with the currently typical acquisition frequencies results in a limited number of samples (10 to 20) per measurement. It is investigated what the effect of limited temporal sampling is on the accuracy of the measured heat flux and guidelines are given for the minimum acquisition frequency. Secondly, due to the improvement in sensor technology, the sensor size has increased resulting also in an increase in the spatial resolution to a point where the smallest detectable heat flux features may become affected by lateral conduction.

2. Classification of unsteady data reduction procedures

In the paper by Walter and Scott (1998), the unsteady data reduction procedures are categorized into three different classes. The methods in class 1 are analytical techniques, which provide a closed form solution of the unsteady conduction equation. The two most important methods in this class are the approaches proposed by Cook & Felderman (1966) and Kendall & Dixon (1967), both are based on the one-dimensional unsteady conduction equation. Elaborations on these methods to include the effect of lateral conduction were later proposed by Estorf (2006) and Liu et al. (2011).

Where the first class methods expressed the resulting surface heat flux in a closed form, the class 2 methods use direct numerical techniques. The benefit of this approach is the increased flexibility when solving the unsteady

conduction equation (e.g. including variable thermal properties of the material) although at the cost of increasing uncertainties. Finally the class 3 methods encompass the full inverse approach, where maximum flexibility is achieved and a multidimensional analysis is possible.

In addition to the class 1 to 3 methods also a class 0 method can be identified. Although this method is not included in the discussion of the Walter and Scott, it should be included here for completeness. In this approach the closed form analytical solution of the unsteady conduction equation with constant surface heat transfer coefficient is used. In the process the analytical solution curve is fitted to the measured surface temperature signal by varying the heat transfer coefficient h and possibly also the adiabatic wall temperature T_{aw} in the process. A major benefit of this approach is that it is rather insensitive to measurement noise, however it only works with steady flows that are governed by a constant heat transfer coefficient and adiabatic wall temperature. For a more elaborate description of this approach the reader is referred to the paper of de Luca et al. (1995).

3. Data reduction procedures

The above described methods increase in complexity (and are generally more computational intensive) when going from class 0 to 3. However the higher-class methods also allow for more flexibility such as the inclusion of variable thermal properties or multidimensional analysis. In the current analysis three methods are investigated more in detail. The first two are the Cook & Felderman (CF) and Kendall & Dixon (KD) algorithms, both are class 1 methods and they are selected here because they are simple to implement while still being rather flexible making them a preferred approach in most aerospace related studies. The third is a class 3 method that is much more complex and is more computational intensive, however it is also the most flexible and should represent the state of the art.

The Cook & Felderman (1966) relation represents a numerical approximation of the integral solution to the unsteady conduction equation where the temperature signal is assumed to be piecewise linear. The surface heat flux is given by:

$$q_{s,\mathrm{C\&F}} = \frac{2\sqrt{\rho c k}}{\sqrt{\pi}} \sum_{j=1}^{n} \frac{\theta_j - \theta_{j-1}}{\sqrt{t_n - t_j} + \sqrt{t_n - t_{j+1}}} \tag{1}$$

It turns out that the Cook & Felderman relation is rather sensitive to the noise levels that are present in the measurement data. This effect can be mitigated using an approach that first computes the cumulative heat input, which was proposed by Kendall & Dixon (1967):

$$Q_{s,\mathrm{K\&D}} = \frac{\sqrt{\rho c k}}{\sqrt{\pi}} \sum_{j=1}^{n} \frac{\theta_j + \theta_{j-1}}{\sqrt{t_n - t_j} + \sqrt{t_n - t_{j+1}}} \Delta t \tag{2}$$

Finally the heat flux is computed by taking the derivative w.r.t time:

$$q_{s,\mathrm{K\&D}} = \frac{dQ_{s,K\&D}}{dt} \tag{3}$$

Depending on the desired smoothness and susceptibility to noise either a broad or narrow differencing scheme can be utilized. In this paper centered differences are used.

The inverse adjoint technique is essentially an optimization process. A surface heat flux variation in time and space is assumed and the surface temperature is calculated by means of a fully implicit finite volume solver, which is compared to the measured surface temperature. In the iterative process the heat flux is adjusted in such a way that the computed surface temperature approaches the measured temperature. In practice the presence of measurement noise may lead to instabilities hence the method is mathematically classified as ill posed. For the solution to be stable, a regularization technique must be applied to the optimization process. In the current approach the iterative regularization principle is applied which uses a suitable choice of the stopping criteria for the iterations such that the final solution is stabilized with respect to the measurement errors. The iterative process uses a conjugate gradient method (CGM) that consists of the following parts (Özisik and Orlande, 2000):

- Adjoint problem; computation of direction of descent
- Sensitivity problem; computation of step size in the direction of descent
- Direct problem; computation of the surface temperature to check for convergence

In practice the following cost functional is minimized for the computed and measured temperature distribution:

$$J[\hat{q}(x,t)] = \int_0^t \sum_{i=1}^{m} [T_i(t) - \theta_i(t)]^2 \, dt \tag{4}$$

Here θ_i is the measured temperature and T_i is the temperature computed from the boundary condition $\hat{q}$. The CGM consists of the following iterative procedure for the heat flux estimate:

$$\hat{q}^{n+1}(x,t) = \hat{q}^{n+1}(x,t) - \beta^n d^n(x,t)\,, \tag{5}$$

where β_n is the search step size obtained through the adjoint problem and d_n is the direction of descent computed from the sensitivity problem. The iterative process is repeated until convergence is reached, in practice this means that the process is stopped when the value of the cost functional J becomes comparable to the noise level that is expected from the measurement (e.g. NETD).

The mesh that is used in the computations is twice the thermal penetration depth ($d = 8\sqrt{\alpha t}$) in order to satisfy the infinite slab boundary condition. The typical mesh size is 100 cells in depth direction; from a grid convergence study it was found that a mesh size larger that 50 cells in depth did not influence anymore the solution.

4. Temporal resolution, effect of limited sample numbers

To investigate the accuracy of each technique in relation to limited temporal sampling, the response of each algorithm is computed for a step-wise variation of the surface heat flux: at *t=0* a heat flux is applied that is constant in time. The result for each method is shown in figure 1 and as reference the exact solution is shown alongside.

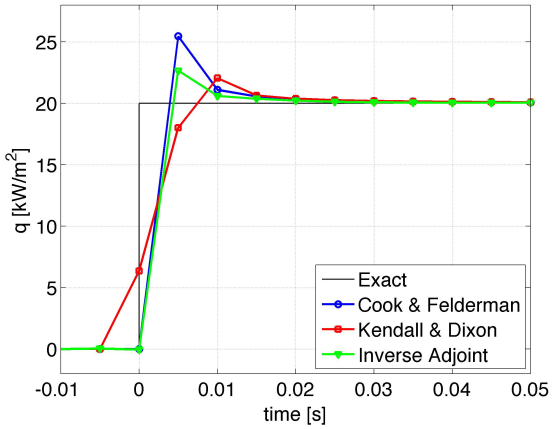

Fig. 1. *Results from different inverse technique for a stepwise variation of the surface heat flux*

It is clearly observed that each technique shows an overshoot at the moment when the surface heat flux has become non-zero. The Cook & Felderman algorithm shows the largest overshoot followed by the inverse adjoint and the Kendall & Dixon approach. Due to the usage of central differences in the Kendall & Dixon method, the gradient of the heat flux is smeared out at *t = 0*. For the Cook & Felderman method one can easily determine the exact amplitude of the overshoot: first, equation (1) is evaluated for the first non-zero contribution of the temperature signal:

$$q_{s,\mathrm{C\&F}} = \frac{2\sqrt{\rho c k}}{\sqrt{\pi}} \frac{\Delta\theta}{\sqrt{\Delta t}} \tag{6}$$

However, according to the exact algebraic solution the surface heat flux is equal to:

$$q_{s,\mathrm{exact}} = \frac{\sqrt{\rho c k}\sqrt{\pi}}{2} \frac{\theta}{\sqrt{t}} \tag{7}$$

Since we are considering the first non-zero entry, $t = \Delta t$ and $\theta = \Delta\theta$ and equations (6) and (7) can be compared which shows that the Cook & Felderman technique always has an overshoot of 27% with respect to the actual heat flux:

$$\frac{q_{s,\mathrm{C\&F}}}{q_{s,\mathrm{exact}}} = \frac{4}{\pi} \tag{8}$$

The error for each method due to the overshoot is shown in figure 2 for *t > 0*. It is found that approximately 6 measurement points are needed such that the error has decreased below 1%, while for the inverse approach this happens after 5 measurement points. Although the errors seem to become acceptable after multiple time-steps (for all

methods the error has dropped below 5% for 3 steps and more) one should keep in mind than for an actual measurement the heat flux is affected by measurement noise and is never constant and therefore is continuously influenced by the overshoot phenomena. This is especially true in cases when the acquisition frequency is limited causing a rather coarse sampling of the temperature signal.

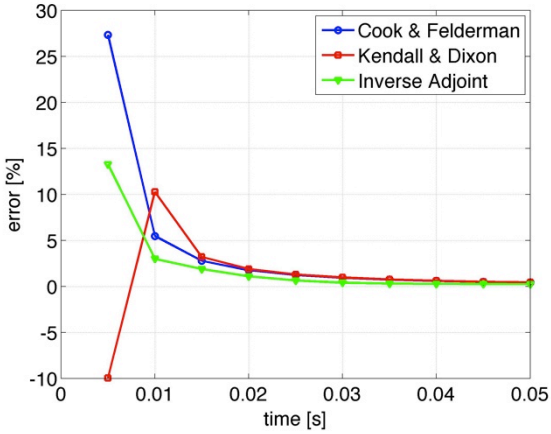

Fig. 2. *Error for the different inverse techniques (only the points for t > 0 are included)*

5. Spatial resolution, effect of lateral conduction

In order to compute the modulation due to effect of lateral conduction, a heat flux is assumed that has a sinusoidal variation in space and is constant in time:

$$q_s = q_0 \sin\left(\frac{2\pi x}{\lambda}\right) \tag{9}$$

For different wavelengths λ the temperature signal is computed using an implicit finite volume solver. The temperature values are then compared to the temperature signal for which there is no lateral conduction. The same approach is taken for the surface heat transfer: the values resulting for the Cook & Felderman method (which does not take into account lateral conduction) are compared to the exact values. The wavelength is non-dimensionalized using the penetration depth as it is defined by Schultz & Jones (1973):

$$\chi = \frac{\lambda}{x_p} = \frac{\lambda}{4\sqrt{\alpha t}} \tag{11}$$

An alternative way of non-dimensionalisation can be performed using the modified Fourier number $Fo = (2\pi/\lambda)^2 \alpha t$ as introduced by de Luca et al. (1991). The relation between χ and the modified Fourier number is:

$$\chi = \frac{\pi}{2}\frac{1}{\sqrt{\mathrm{Fo}}} \tag{12}$$

The advantage of using χ instead of *Fo* is that it directly relates a length scale for the lateral conduction to the length scale appropriate for normal conduction.

Figure 3a shows the temperature and heat flux modulation as a function of χ and in figure 3b as a function of λ. The temperature modulation function as function of the modified Fourier number is in fact identical to the Temperature Amplitude Transfer Function that is introduced by de Luca et al. (1991).

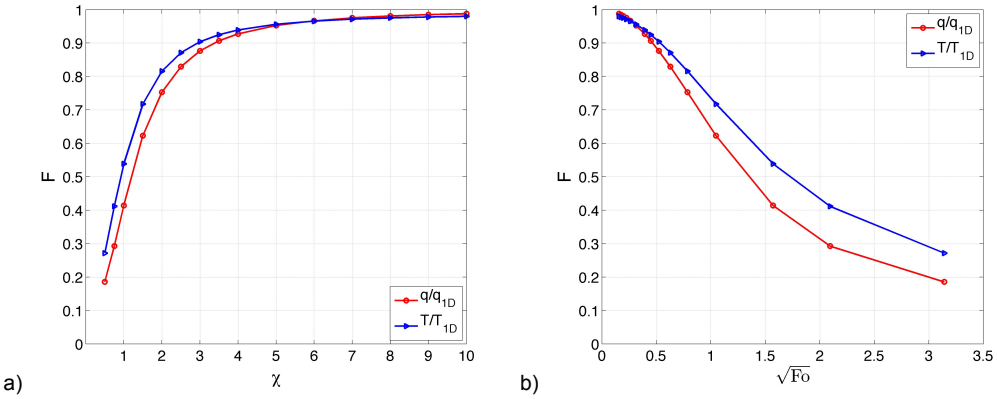

Fig. 3. *Modulation of the surface heat flux and surface temperature due to lateral conduction, a) as a function of χ and b) as a function of $\sqrt{\mathrm{Fo}}$*

It is apparent from the figure that the modulation increases with decreasing χ and increasing *Fo* (smaller wavelengths). Furthermore it is found that the modulation is stronger for the heat flux than for the temperature although the difference is not very large. On overall it can be concluded that a 10% modulation error is expected for non-dimensional wavelengths for which $\chi < 3.5$ (or $Fo > 0.2$). This observation can now be used to define a relation between the total measurement time t_{max} and the minimum detectable wavelength λ_{min} for which the modulation is less than 10%:

$$\lambda_{\min} > 14\sqrt{\alpha t_{\max}} \tag{13}$$

In table 1, some typical values for the minimum wavelength and maximum measurement time are summarized for different materials. In the third column the minimum wavelength for which the modulation error is less than 10% for a measurement time of 1 second is given. It can be seen that when performing a transient measurement on a Makrolon surface with a maximum duration of 1 second, lateral conduction effects affect all heat flux features that have a typical wavelength smaller than 5 mm. As expected for stainless steel and copper these values are even bigger. In the last column the maximum measurement time is indicated for a minimum wavelength of 2 mm. This value is chosen because it is the typical minimum wavelength that can be resolved by a standard IR camera with an objective of 25 mm while taking into account the Nyquist criterion and the camera modulation transfer functions. From the values in the table can be concluded for short duration facilities that operate in the milliseconds to seconds range, materials should be selected that have a thermal diffusivity that should not exceed the one of Makrolon such as not to be biased due to lateral conduction effects.

Table 1. *Minimum detectable wavelength and maximum measurement time due to lateral conduction for different materials*

Material	Diffusivity [m^2/s]	λ_{min} [*mm*] for t = 1 *s*	t_{max} [*ms*] for λ_{min} = 2 *mm*
Makrolon	1.4×10^{-7}	5.2	150
Stainless Steel	4.2×10^{-6}	28.7	4.9
Copper	1.1×10^{-4}	146.8	0.19

6. Experimental results

To investigate the performance of these methods under real experimental conditions, they are applied to an experimental data set of a hypersonic flow in a short duration facility at Mach 7.5 with a typical run-time of 0.1 s. The objective of the investigation was to study the development of Görtler vortices over a double compression ramp. The IR images were recorded by means of a Cedip Titanium 530L camera with a 25 mm objective. The spatial resolution was approximately 0.6 mm/pixel and the integration time was set to 72 µs. For more information concerning the experiments the reader is referred to Schrijer (2011). In figure 4 a top-view of the wind tunnel model is shown (flow direction is from bottom to top) where the colors represent the temperature increase since the start of the wind tunnel run. Near the nose a comb-shaped element is placed that produces vortices which explains the streamwise streaks that are present in the thermogram. Due to these vortices, spanwise temperature gradients are generated that may cause lateral heat conduction and therefore presents a good testcase.

http://dx.doi.org/10.21611/qirt.2012.317

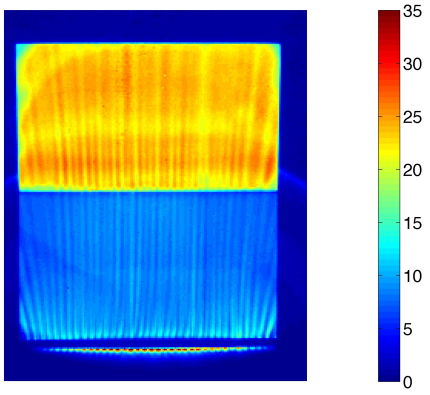

Fig. 4. *Thermogram of the wind tunnel model at t = 0.09 s. The colorbar indicates the temperature increase since the start and the flow is from bottom to top.*

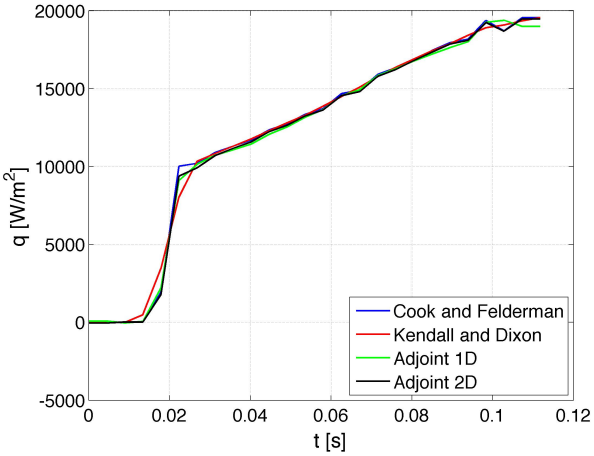

Fig. 5. *Spanwise average heat flux variation with time at 5 mm downstream of the comb-shaped element*

In figure 5 the average spanwise heat flux is show at 5 mm downstream of the comb-shaped element. From the figure it is clear that the heat flux is not constant and that it increases over time. Just before t = 0.02 the wind tunnel starts and the heat flux increases. When comparing the different methods it can be observed that Cook & Felderman shows the largest 'overshoot' while for Kendall and Dixon it is the least, although the magnitude is negligible. When progressing further in time, the heat flux values returned by the various methods are practically the same.

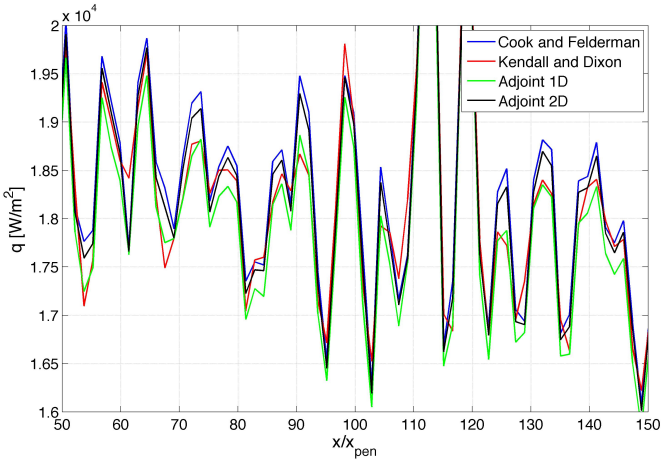

Fig. 6. *Spanwise heat flux profile at 5 mm downstream of the comb-shaped element (x_{pen} = 0.46 mm).*

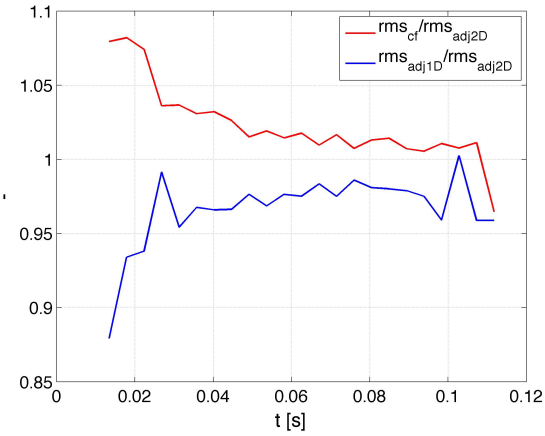

Fig. 7. *Spanwise rms heatflux at 5 mm downstream of the comb-shaped element.*

Observing the spanwise variation in the heat flux (figure 6), the footprint of the vortices is clearly observed. In the figure the results for Cook & Feldermann and Kendall & Dixon are plotted, and the results from the adjoint technique applied to a 1D and to a 2D mesh are shown as well. Naturally, the 1D adjoint does not take into account the effects of lateral conduction. The horizontal axis is non-dimensionalized with the penetration depth and it can be seen that the typical wavelength is approximately $\lambda/x_{pen} = \chi \approx 6$. From figure 3a it can be seen that for this non-dimensional wavelength a typical modulation around 0.95 can be expected. Now when returning to figure 6 and comparing the curves it becomes apparent that the largest fluctuations are observed for Cook & Feldermann followed by the 2D adjoint technique. To quantify the difference measured in heat flux amplitude, the ratio of rms fluctuations along the span is plotted for CF and 2D adjoint and 1D and 2D adjoint in figure 7. When comparing 1D to 2D adjoint it can be seen that the 1D adjoint returns a heat flux amplitude that is 0.97 – 0.98 that of the 2D adjoint, which is mainly attributed to the fact that the 1D adjoint does not take into account lateral conduction. However when CF is compared to 2D adjoint it can be concluded that the fluctuations returned by CF are consistently larger, which is contrary to what is expected because the CF method is purely 1D. Although this is not confirmed it is believed that the difference can be attributed to the presence of measurement noise, more investigation of this matter is needed. Furthermore it can be observed that the ratio between rms CF and rms 2D adjoint decreases over time, which is a direct effect of including lateral conduction in the 2D adjoint method.

7. Conclusions

Two effects were investigated that may have an important influence on transient infrared measurements and heat flux data reduction: limited temporal sampling and the effect of lateral conduction. In combination a total of three different data reduction methods were tested: two methods that are based on the 1D assumption (Cook & Feldermann and Kendall & Dixon) that are easy to implement but not so flexible and an 2D adjoint technique that is more complex to implement but much more flexible and capable to take into account the effect of lateral conduction.

The effect of limited temporal sampling was investigated by means of a stepwise heat flux test case and it can be concluded that for a constant heat flux in absence of noise, a sampling of the transient with 5 to 6 points depending on the data reduction method is sufficient to decrease the error below 1%. However the effect of (small) heat flux variations and the presence of measurement noise in real experiments may require having at least 10 to 20 data points during a test run. For the Cook & Feldermann method a rather large (27%) overshoot was observed at the first time-step while for the adjoint method it was lower (approx. 13%).

Furthermore from synthetic simulations it was found that heat flux features containing spatial wavelengths that are smaller than 3.5 times the penetration depth are affected by lateral conduction and that therefore the results become modulated when using data reduction models based on the 1D semi-infinite slab assumption.

Finally the three methods were applied to an experimental test case in order to observe the above-mentioned effects. A small overshoot was observed for both the Cook & Feldermann and adjoint technique, however the value of the overshoot was practically negligible. Also the lateral conduction corrections that were expected when using a 2D adjoint method were not as evident. This was caused by two effects; first, the spatial wavelengths in the temperature signal were rather large such that the improvement by including the lateral conduction term is limited. Furthermore the combination of a non-constant heat flux in time with measurement noise, which was not taken into account in the theoretical analysis may have a large effect on the final results.

Concluding can be remarked that further investigation is needed into the effects of variable heat flux and measurement noise. Also a better suited experiment is required such that experimental data is acquired at smaller wavelengths where the effect of lateral conduction becomes more pronounced.

REFERENCES

[1] Levesque P., Brémont P., Lasserre J.L., Paupert A. and Balageas D.L., “Performance of FPA IR cameras and their improvement by time, space and frequency data processing. Part I – Intrinsic characterization of the thermographic system”. QIRT Journal, vol. 2, pp. 97 – 112, 2005.

[2] Pron H. and Bissieux C., “Focal plane array infrared cameras as research tools”. QIRT Journal, vol. 1, pp. 229 – 240, 2004.

[3] Poncelet M., Witz J.-F., Pron H. and Wattrisse B., “A study of IRFPA camera measurement errors: radiometric artefacts”. QIRT Journal, vol. 8, pp. 3 – 20, 2011.

[4] de Luca L. and Cardone G., “Modulation transfer function cascade model for a sampled IR imaging system”. Applied Optics, vol. 30, no. 13, pp. 1659 – 1664, 1991

[5] George W.K., Rae W.J. and Woodward S.H., “An evaluation of Analog and Numerical Techniques for Unsteady Heat Transfer Measurement with Thin-film Gauges in Transient Facilities”. Experimental Thermal and Fluid Science, vol. 4, pp. 333 – 342, 1991.

[6] Walker D.G. and Scott E.P., “Evaluation of Estimation Methods for High Unsteady Heat Fluxes from Surface Measurements”. Journal of Thermophysics and Heat Transfer, vol. 12, no. 4, pp. 543 – 551, 1998

[7] Cook W.J. and Felderman E.J., “Reduction of Data from Thin-Film Heat-Transfer Gages: A Concise Numerical Technique”. AIAA Journal, vol. 4, no.3, pp. 561 – 562, 1966

[8] Kendall D.N., Dixon W.P. and Schulte E.H., “Semiconductor Surface Thermocouples for Determining Heat Transfer Rates”. IEEE Transactions on Aerospace and Electronic Systems, vol. AES-3, no. 4, 1967.

[9] de Luca L., Cardone G., Aymer de la Chevalerie D. and Fonteneau A., ”Viscous Interaction Phenomena in Hypersonic Wedge Flow”. AIAA Journal, vol. 33, no. 12, pp. 2293 – 2298, 1995.

[10] Özisik M.N. and Orlande H.R.B, “Inverse Heat Transfer – Fundamentals and Applications”. Taylor & Francis, New York, 2000.

[11] Schultz D. and Jones T.V., “Heat Transfer Measurements in Short Duration Hypersonic Facilities”. AGARDograph, TR165, 1973.

[12] Schrijer F.F.J., “Investigation of Görtler vortices in a hypersonic double compression ramp flow by means of infrared thermography”. QIRT Journal, vol. 7, pp. 201 – 215, 2010.